CASL-U-2014-0123-000-a

Power uprates and plant life extension

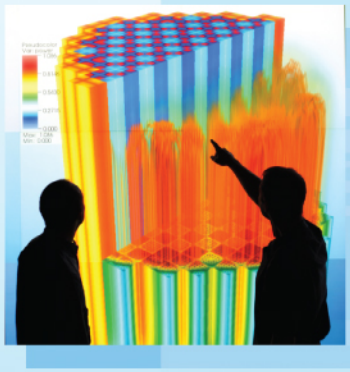

Engineering design and analysis

Science-enabling high performance computing

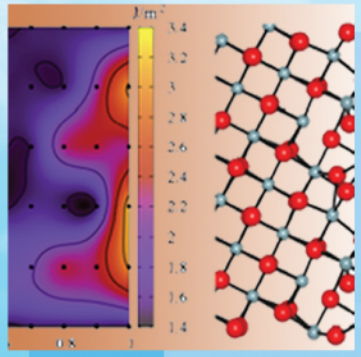

Fundamental science

Plant operational data

Consortium for Advanced Simulation of LWRs

L3:RTM.SUP.P9.01

Resonance Self-shielding Method for Fuel Annular Subdivisions Using Quasi-1D Slowing-down Solution

Yuxuan Liu and William Martin University of Michigan

Mark Williams and Kang-Seog Kim
Oak Ridge National Laboratory

July 31, 2014

U.S. DEPARTMENT OF ENERGY | Nuclear Energy

CASL-U-2014-0123-000-a

Resonance Self-shielding Method for Fuel Annular Subdivisions Using Quasi-1D Slowing-down Solution

Yuxuan Liu and William Martin
Department of Nuclear Engineering and Radiological Sciences, University of Michigan
2355 Bonisteel Blvd., Ann Arbor, MI, 48109

Mark Williams and Kang-Seog Kim
Oak Ridge National Laboratory
One Bethel Valley Road, P.O. Box 2008, Oak Ridge, TN 37831-6172, USA

47 pages

1 title page

1 abstract page

30 pages of manuscript

9 pages of 9 figures

6 pages of 6 tables

Corresponding Author:

Yuxuan Liu

Email:

yuxuanl@umich.edu

Mailing address:

2355 Bonisteel Blvd.
1906 Cooley Building
Ann Arbor, Michigan 48109-2104

CASL-U-2014-0123-000-a

ABSTRACT

A correction-based resonance self-shielding method is developed that allows annular subdivision of the fuel rod. The method performs the conventional iteration of the embedded self-shielding method (ESSM) without subdivision of the fuel to capture the inter-pin shielding effect. The resultant self-shielded cross sections are modified by correction factors incorporating the intra-pin effects of radial variation of the shielded cross section, radial temperature distribution and resonance interference. A quasi-1D slowing-down equation is developed to calculate such correction factors. The method is implemented in the DeCART code and compared with the conventional ESSM and subgroup method with benchmark MCNP results. The new method yields substantially improved results for both spatially dependent reaction rates and eigenvalues for typical PWR pin cell cases with uniform and non-uniform fuel temperature profiles.

Keywords: spatial self-shielding with non-uniform temperature; ESSM; resonance interference.

I. INTRODUCTION

When deterministic neutron transport methods are applied to lattice or whole-core problems, the multi-group approximation is usually applied to the cross section treatment for the energy domain. Due to the complicated energy behavior of resonance cross sections, the weighting spectrum for collapsing multi-group cross sections is very dependent on energy and space, which becomes a crucial challenge when analyzing a lattice or full-core configuration. There are generally two groups of approaches to perform the resonance self-shielding calculation. The first one is to solve the slowing-down equations for the problem of interest using continuous-energy (CE) or ultrafine-group cross sections in order to account for these resonance phenomena. Because of the computational burden, slowing-down codes are restricted to local geometries such as pin cells or assemblies. For example, RMET21 [1] and the early version of CENTRM [2] are restricted to 1-D cylindrical pin cell geometry that has been converted from the square pin cell using the Wigner-Seitz approximation. The MERIT [3] code analyzes a 2-D pin cell calculation using the Method of Characteristics (MOC), which removes the possible error arising from the Wigner-Seitz approximation. Recently, this 2-D pin cell capability has been included in the latest version of CENTRM [4]. To account for the inter-pin heterogeneity, a 2-D slowing-down code for assembly calculation is first attempted in the GEMINEWTRN code [5]. The self-shielded cross sections can be accurately generated by GEMINEWTRN with regard to the spatial heterogeneity, but the computing time becomes an issue when the assembly-size problem is solved by the direct slowing-down method. Currently, solving the slowing-down equation for a 2-D full core problem is still computationally prohibited, so the influence of neighboring assemblies or reflector regions on the shielded cross sections is hardly being considered by direct slowing-down method.

The second group of approaches for resonance self-shielding calculation utilizes pre-computed integral tables. Under the most circumstance, resonance integral (RI) tables are generated. To

compute RI tables, the slowing-down equation is solved over the range of a parameter called background cross section which is a measure of dilution. The Bondarenko method [6] is a conventional approach correlating RI and background cross section. Based on the equivalence theory [7], the heterogeneous self-shielding effect can be modelled by including an equivalence cross section into the background cross section, and variations of Bondarenko method were developed to treat heterogeneity [7,8]. In the past two to three decades, a powerful alternative of the Bondarenko method, the subgroup method [9,10] has been developed and widely implemented in modern lattice codes. In the subgroup approach, the detailed cross section behavior of each coarse energy group is replaced by its probability density representation preserving certain integrals. There are two groups of methodologies for determining the subgroup probability tables [11]. The first one is the physical probability table, in which the RI tables are converted into a set of subgroup levels and weights by preserving RI or effective cross section over different background cross sections. The second one is the mathematical probability table. Instead of preserving resonance integral, it preserves the cross section moments by processing the point-wise cross section data. Recently another promising RI table based method, the iterative self-shielding method [12,13] was developed by Korea Atomic Energy Research Institute (KAERI) and Oak Ridge National Laboratory (ORNL). ORNL entitled it the Embedded Self-Shielding Method (ESSM) because compared to the conventional Bondarenko method in which the Dancoff factor is usually evaluated outside the transport calculation, ESSM provides tighter coupling between the neutron transport and self-shielding calculations, assuring that the heterogeneous self-shielding effects are consistent with the multi-group transport calculations of the system.

Since the application of integral table based methods only involve multi-group calculation, these methods are much more efficient than directly solving the CE slowing-down equation for the specific configuration. However, integral table based methods have their own issues. First, the

integral tables are generally determined for each resonance isotope independently, so resonance interference is neglected at this step and treated afterwards at the multi-group level, e.g., using Bondarenko iteration as described in the WIMS code [8]. Nevertheless, it is shown in early research by Williams that the corrections for interference effect in the multi-group framework cannot resolve various conditions of the resonance overlap for a mixture of resonance isotopes [14]. Alternatively, efforts were made to incorporate the interference effect by extending the dimension of RI table or subgroup parameters using the density ratio of two resonance isotopes [15,16]. Difficulty for these methods occurs when the number of resonance isotopes becomes large, e.g. for MOX fuel or depleted fuel. An increasing size of RI table has to be determined depending on the number and significance of the resonance isotopes in the specific problem, which is practically inefficient. The second issue of integral table based method is the spatial self-shielding within the fuel region. The Bondarenko method and ESSM primarily rely on the equivalence theory, which was conventionally developed for a single fuel region without subdivision. However, high-fidelity reactor simulations of today require a resonance self-shielding model which is able to resolve the spatial effects within the fuel rod for multi-region depletion and power density calculation [17]. There have been a few efforts to develop spatially-dependent self-shielding models [18,19,20] in the framework of the Bondarenko method. The multiple fuel region escape probability is calculated by either extending the rational type approximation or rigorous computation from the point-wise cross section data. The shielded cross sections are still represented in terms of resonance integral, with extra coefficients accounting for the spatial effects. Limitation of these models is the absence of treatment for the non-uniform temperature distribution throughout the fuel rod. For the conventional lattice calculation, a so called ‘effective temperature’ (single value) is chosen to replace the realistic temperature distribution in the fuel rod. Various approaches to obtain the effective temperature were discussed in Ref. [21]. The concept behind these approaches is to conserve the neutron absorption of a non-uniform temperature profile with that of the effective temperature. Apparently, the effective

temperature model cannot be used with radially dependent temperatures if one wants to obtain accurate self-shielded cross sections in every sub-region of the fuel. Although the subgroup method reduces the dependence on equivalence theory, which leads to a better representation of spatial self-shielding, the lack of theoretical foundation in treating non-uniform temperature restricts its applicability, particularly to the direct whole core problems with thermal feedback. Prescriptions to this theoretical deficiency were presented in Ref. [22,23] to improve the accuracy of fuel temperature coefficient, but no detailed comparisons of the spatially dependent reaction rates with regard to the non-uniform temperature profiles were provided. Additionally, the problem becomes more difficult if the resonance interference effect is also considered in the spatially self-shielding calculations.

A new correction-based method [24,25] was devised to resolve the resonance interference effect explicitly for a mixture of resonance isotopes by utilizing ESSM and 0-D slowing-down calculation, respectively. However, this approach was restricted to a single fuel region. Motivated by the success of the correction method using the slowing-down solution, a comprehensive method is developed in this paper to account for all three issues i.e., resonance interference, spatial self-shielding, and non-uniform temperature profile. The method incorporates continuous energy (pointwise cross section) slowing-down model. A quasi-1D slowing-down equation is developed where the equivalence cross section is allowed to be energy dependent. Correction factors are computed by comparing the self-shielded cross sections of the subdivided fuel pallet with a single-region fuel pallet, using the quasi-1D slowing-down calculation to compute both sets of shielded cross sections. ESSM is still performed to generate the base shielded cross sections with single fuel regions for the global geometry. These shielded cross sections are then modified by the correction factors that depend on the fuel sub-regions. The theoretical foundation for the model will be discussed first, followed by the numerical verifications.

II. THEORY

This section consists of three parts. First, the fundamentals of ESSM and associated RI tables are discussed, followed by the derivation of the quasi-1D slowing-down equation for efficient calculation of the correction factors. This section concludes with a description of how the correction factors are applied.

II.A. ESSM and RI tables

ESSM is fundamentally a variation of the extensively used Bondarenko method [12,13]. It evaluates the equivalence cross section by performing iterations between the calculation of the self-shielded cross sections and the fixed-source transport problem for the geometry and composition of interest, typically a 2-D plane of the core and reflector. The subgroup approach also uses 2-D fixed-source transport solutions to evaluate the subgroup-level dependent equivalence cross sections. Thus ESSM avoids the complicated generation of subgroup levels and weights, although this is only done once for a given library. Next, the ESSM and associated RI tables are consistently derived.

Generally, the goal of resonance calculation is to evaluate multi-group self-shielded cross section $\sigma_{x,g}$ for resonance isotopes at reaction channel *x* in energy group *g* with group width Δu_g ,

$$\sigma_{x,g}(r) = \int_{\Delta u_g} \sigma_x(u)\phi(r,u)du \Big/ \int_{\Delta u_g} \phi(r,u)du \tag{1}$$

where $\phi(r,u)$ is the neutron flux at spatial location *r* for lethargy *u*. For the best accuracy of the resonance energy range, the weighting flux $\phi(r,u)$ in Eq. (1) should be the solution of the neutron slowing-down equation for the specific problem being analyzed. Denote $\boldsymbol{F}$ as fuel material and $\boldsymbol{M}$ as a material other than fuel (cladding, coolant, etc.). Assuming a single fuel

region without subdivision, the collision probability form of the slowing-down equation is given as

$$V_F \Sigma_{t,F}(u)\phi_F(u) = V_F P_{F\to F}(u) Q_F(u) + \sum_{J\in M} V_J P_{J\to F}(u) Q_J(u) \tag{2}$$

where V_F , $\Sigma_{t,F}(u)$ and $\phi_F(u)$ are the volume, total cross section and scalar flux of the fuel, respectively. $P_{F\to F}(u)$ and $P_{J\to F}(u)$ are the first flight collision probabilities from fuel to fuel and from material *J* to fuel. The source term $Q_F(u)$ can be explicitly written as

$$Q_F(u) = \sum_{iso} \int_{u-\varepsilon_{iso}}^{u} \Sigma_{s,F,iso}(u')\phi_F(u') \frac{e^{u'-u}}{1-\alpha_{iso}} du' \tag{3}$$

where ε_{iso} and α_{iso} are the maximum lethargy gain and the fractional energy loss when a neutron scatters off isotope *iso,* and $\Sigma_{s,F,iso}$ is the scattering cross section of isotope *iso* in the fuel. As in the resonance energy range, three major assumptions underpin Eq. (3): (a) the scattering source is isotropic in the center-of-mass system, and includes only s-wave elastic reactions; (b) up-scattering is neglected; and (c) the direct fission source is neglected. To proceed, the Intermediate Resonance (IR) approximation [26] is applied to the fuel material to obtain

$$Q_F(u) = \sum_{iso} \lambda_{iso} \Sigma_{p,F,iso} + \sum_{iso} (1-\lambda_{iso}) \Sigma_{s,F,iso}(u)\phi_F(u) \approx \lambda_F \Sigma_{p,F} + (1-\lambda_F)\Sigma_{s,F}(u)\phi_F(u) \tag{4}$$

where $\Sigma_{p,F,iso}$ denotes the potential scattering cross section and λ_{iso} is the IR factor, where the notation is then simplified by dropping the isotope index. The scattering source for materials other than fuel can be written in a similar form as Eq. (3), but with the Narrow Resonance (NR) approximation,

$$Q_J(u) = \Sigma_{p,J} \quad \left(J \in M\right) \tag{5}$$

Substitution of Eqs. (4) and (5) into Eq. (2) for $Q_F(u)$ and $Q_J(u)$ yields

$$V_F\Sigma_{t,F}(u)\phi_F(u) = V_F P_{F\to F}(u)\left[\lambda_F\Sigma_{p,F} + (1-\lambda_F)\Sigma_{s,F}(u)\phi_F(u)\right] + \sum_{J\in M} V_J P_{J\to F}(u)\Sigma_{p,J} \quad (6)$$

Assuming $\Sigma_{t,J}(u) = \Sigma_{p,J}$ for the non-fuel materials and using the reciprocity relation, $V_X P_{X\to Y}(u)\Sigma_{t,X}(u) = V_Y P_{Y\to X}(u)\Sigma_{t,Y}(u)$, Eq. (6) can be transformed into

$$\Sigma_{t,F}(u)\phi_F(u) = \left(1-P_{esc}(u)\right)\left[\lambda_F\Sigma_{p,F} + (1-\lambda_F)\Sigma_{s,F}(u)\phi_F(u)\right] + \Sigma_{t,F}(u)P_{esc}(u) \quad (7)$$

where the escape probability is defined as $P_{esc}(u) = \sum_{J\in M} P_{F\to J}(u)$. Based on the conventional equivalence theory, the escape probability can be written as a single-term rational form

$$P_{esc}(u) = \frac{\Sigma_e}{\Sigma_{t,F}(u) + \Sigma_e} \quad (8)$$

By applying Eq. (8), the fuel flux in Eq. (7) becomes

$$\phi_F(u) = \frac{\lambda_F\Sigma_{p,F} + \Sigma_e}{\Sigma_{t,F}(u) - (1-\lambda_F)\Sigma_{s,F}(u) + \Sigma_e} \quad (9)$$

If the scattering cross section term is split into potential and resonance parts, i.e. $\Sigma_{s,F}(u) = \Sigma_{RS,F}(u) + \Sigma_{p,F}$,

$$\phi_F(u) = \frac{\lambda_F\Sigma_{p,F} + \Sigma_e}{\Sigma_{a,F}(u) + \lambda_F\Sigma_{RS,F}(u) + \lambda_F\Sigma_{p,F} + \Sigma_e} \quad (10)$$

As usual, the summation of energy-independent terms are defined as the background cross section

$$\phi_F(u) = \frac{\Sigma_b}{\Sigma_{a,iso}(u) + \lambda_{iso}\Sigma_{RS,iso}(u) + \Sigma_b} \quad or \quad \phi_F(u) = \frac{\sigma_{b,iso}}{\sigma_{a,iso}(u) + \lambda_{iso}\sigma_{RS,iso}(u) + \sigma_{b,iso}} \quad (11)$$

where $\Sigma_b = \lambda_F \Sigma_{p,F} + \Sigma_e$, $\sigma_{b,iso} = \Sigma_b / N_{iso}$ and N_{iso} is the number density of resonance isotope *iso*. Eq. (11) assumes no resonance interference among resonance isotopes so the microscopic cross sections in the denominator pertain only to resonance isotope *iso*. Applying Eq. (11) to Eq. (1) indicates that the shielded cross section is only dependent on the background cross section

$$\sigma_{x,iso,g} = \frac{\int_{\Delta u_g} \sigma_{x,iso}(u) \dfrac{\sigma_{b,iso}}{\sigma_{a,iso}(u) + \lambda_{iso}\sigma_{RS,iso}(u) + \sigma_{b,iso}} du}{\int_{\Delta u_g} \dfrac{\sigma_{b,iso}}{\sigma_{a,iso}(u) + \lambda_{iso}\sigma_{RS,iso}(u) + \sigma_{b,iso}} du} \tag{12}$$

Given the connection between shielded cross section and background cross section, the slowing-down calculations are performed to obtain the self-shielded cross sections for a range of background cross sections. A straightforward way would be to solve the slowing-down equation for a homogeneous mixture of a resonant material and a scattering nuclide whose content can be varied through the background cross section as in the GROUPR module of NJOY [27]. However, a better way is to use a set of heterogeneous pin cell configurations in the realistic reactor geometry by varying the fuel and moderator densities or fuel to moderator ratios to achieve a range of background cross sections. The transition from homogeneous to 1D cylindrical geometry was firstly attempted when performing the verification calculation in Ref. [28] and later this approach was adopted for the generation of subgroup weights in the HELIOS code [29]. Other efforts employing the heterogeneous RI table rather than the homogeneous RI table can be found in Ref. [30,31]. ESSM employs a search for the equivalence cross section by iterating between the pre-computed RI tables and the fixed source problem, and this consistency between generating and using the tables is essential for the accuracy of the method, which is discussed next.

The multi-group form of Eq. (11) can be obtained by first rearranging the denominator to the left hand side, and then integrating over the group boundaries,

$$\phi_{F,g} = \frac{\Sigma_{b,g}\Delta u_g}{\Sigma_{a,iso,g} + \lambda_{iso}\Sigma_{RS,iso,g} + \Sigma_{b,g}} \tag{13}$$

The background cross section can then be solved in terms of the flux

$$\Sigma_{b,g} = \frac{\left(\Sigma_{a,iso,g} + \lambda_{iso}\Sigma_{RS,iso,g}\right)\phi_{F,g}}{\Delta u_g - \phi_{F,g}} \tag{14}$$

The dependence of the shielded cross section versus background cross section can be determined by a series of realistic 2-D pin cell problems with various configurations similar to Ref. [30,31]. For each configuration, the multi-group self-shielded cross sections are computed from the exact 2-D slowing-down calculation. To obtain the corresponding background cross section, the unknown flux in Eq. (14) is solved from a fixed source problem of the same 2-D pin cell configuration formulated using the IR approximation (the multi-group shielded cross sections in the following equation are computed from the exact 2-D slowing-down calculation)

$$\nabla \cdot \Omega\varphi_g(r,\Omega) + \Sigma_{t,g}(r)\varphi_g(r,\Omega) = \frac{1}{4\pi}\left[\left(1-\lambda\right)\left(\Sigma_{RS,g}(r) + \Sigma_p(r)\right)\phi_g(r) + \lambda\Sigma_p(r)\Delta u_g\right] \tag{15}$$

where $\varphi_g(r,\Omega)$ is the angular flux with respect to location r and angle Ω. Therefore, the procedure of generating heterogeneous RI table for ESSM can be summarized as three steps: (a) Solve exact slowing-down equation for every pin cell configuration to obtain the multi-group self-shielded cross sections; (b) Solve Eq. (15) to obtain the scalar flux of the fixed source problem for every pin cell configuration; (c) Obtain the background cross section by Eq. (14) so that the self-shielded cross section and background cross section are linked. This procedure is performed for every resonance isotope at several temperatures of interest.

When performing the resonance calculation of a specific problem, ESSM directly uses these RI tables for cross section interpolation. An initial set of self-shielded cross sections can be

obtained by assuming $\Sigma_e = 0$ so that $\sigma_b = \lambda_F \Sigma_{p,F} \big/ N_{iso}$. With the coefficients of these multi-group shielded cross sections, Eq. (15) is solved for every 2-D plane and the resulting flux is used in Eq. (14) to update the background cross sections. Then a new set of self-shielded cross sections can be obtained by RI table interpolation. The procedure iterates until the equivalence cross sections Σ_e of all resonant regions of the 2-D plane converge.

To be consistent with the generation of the RI tables, the ESSM iteration should be performed for each resonance isotope independently, where other resonance isotopes are treated as background isotopes with only potential scattering. However, because the equivalence cross section for the single fuel region is not very sensitive to the total cross section [32], in order to save computing time, a simplification was introduced by the original presentation of ESSM that the ESSM iteration is performed only once with all the resonance isotopes as a whole absorber. The resonance interference can be considered later by interference models but not confusing the ESSM iteration loop. The correction model discussed in this paper will follow this simplification but cancel out the resultant bias by carefully computing the correction factors. This issue is addressed later in the Section II.C.

Also, it has been verified that $\lambda\Sigma_{RS,g}$ can be eliminated in Eq. (14) and Eq. (15) without sacrificing accuracy, if they are consistently eliminated when generating and using RI tables [29,31]. This can be explained as $\lambda\Sigma_{RS,g}$ only imposes a shift of RI versus background cross sections. By eliminating $\lambda\Sigma_{RS,g}$, Eq. (14) and (15) become

$$\Sigma_{b,g} = \frac{\Sigma_{a,iso,g}\phi_{F,g}}{\Delta u_g - \phi_{F,g}} \tag{16}$$

$$\nabla \cdot \Omega \varphi_g(r,\Omega) + \Sigma_{t,g}(r)\varphi_g(r,\Omega) = \frac{1}{4\pi}\left[\left(\Sigma_{s,g}(r) - \lambda\Sigma_p(r)\right)\phi_g(r) + \lambda\Sigma_p(r)\Delta u_g\right] \tag{17}$$

These two equations are used in the ESSM calculation.

In the foregoing derivation of conventional ESSM, obtaining Eq. (7) and Eq. (8) requires a single fuel region without subdivision. Although one can extend the method to solve a multiple-fuel-region problem by calculating the multi-region fluxes from Eq. (17) and evaluate the background cross sections of different annuli using different fluxes, the same RI table pre-computed from a single fuel region is used for different sub-regions, which prematurely assumes the correlations between shielded cross section and background cross section for different annuli are identical to the single fuel region. This assumption leads to significant errors in the shielded cross sections. Numerical results illustrating this behavior are given later in Section III.

II.B. A quasi-1D slowing down equation

A quasi-1D slowing-down equation is developed in this subsection. The correction factors accounting for the spatial self-shielding, resonance interference, and non-uniform temperature distribution are obtained by solving the quasi-1D slowing-down model with appropriate conditions to account for these effects. Consider a fuel rod which is divided into multiple annuli, where different annuli may have different temperatures and material compositions. The neutron flux in region *i* of the fuel rod is given by the collision probability form of the transport equation with the source term only including scattering (same assumptions for resonance energy range as in the previous subsection)

$$V_i \Sigma_{t,i}(u)\phi_i(u) = \sum_{j\in F} V_j P_{j\to i}(u) Q_j(u) + \sum_{k\in M} V_k P_{k\to i}(u) Q_k(u) \tag{18}$$

where V_i , $\Sigma_{t,i}(u)$ and $\phi_i(u)$ are the volume, total cross section and scalar flux of region *i*. $P_{j\to i}(u)$ is the first flight collision probability from region *j* to *i* and $Q_j(u)$ is the scattering

source of region *j*. Applying NR approximation for the scattering source of the non-fuel regions yields

$$V_i \Sigma_{t,i}(u)\phi_i(u) = \sum_{j\in F} V_j P_{j\to i}(u) Q_j(u) + \sum_{k\in M} V_k P_{k\to i}(u)\Sigma_{p,k} \tag{19}$$

By utilizing the reciprocity relation $V_X P_{X\to Y}(u)\Sigma_{t,X}(u) = V_Y P_{Y\to X}(u)\Sigma_{t,Y}(u)$,

$$\phi_i(u) = \sum_{j\in F} \frac{P_{i\to j}(u)}{\Sigma_{t,j}(u)} Q_j(u) + \sum_{k\in M} P_{i\to k}(u) \tag{20}$$

Earlier spatially dependent self-shielding methods also simplify the source term of the fuel regions using the NR approximation. This approximation is problematic because it gives the same scattering source $Q_j(u)$ for different fuel regions. Although the scattering cross section at lethargy *u* could be same for different fuel regions at uniform temperature and fuel composition, the flux is strongly shielded in the fuel center in comparison to the fuel surface near large absorption resonances, resulting in different scattering sources along the fuel radius. Another approximation of the conventional treatment is assuming the total cross section to be spatially independent, i.e., $\Sigma_{t,j}(u) = \Sigma_{t,F}(u)$. This assumption is poor for at least two cases: depleted fuel and a non-uniform temperature profile. In the following derivation, both of these approximations are removed. The region-to-region collision probability $P_{i\to j}(u)$ is evaluated, but an approximation is introduced to save computing time.

Instead of directly calculating $P_{i\to j}(u)$, we calculate

$$\tilde{P}_{i\to j}(u) = P_{i\to j}^{T_i,C_i}(u) \frac{\sum_{j\in F} P_{i\to j}(u)}{\sum_{j\in F} P_{i\to j}^{T_i,C_i}(u)} = P_{i\to j}^{T_i,C_i}(u) \frac{1-P_{esc,i}(u)}{1-P_{esc,i}^{T_i,C_i}(u)} \tag{21}$$

As shown in Fig. 1, $P_{i\to j}^{T_i,C_i}(u)$ is the first flight collision probability from region *i* to *j* assuming a uniform temperature T_i and material composition C_i throughout the whole fuel. In a media of uniform temperature and material composition, $P_{i\to j}$ can be easily tabulated by the total cross section levels. Thus, in the resonance calculation, $P_{i\to j}^{T_i,C_i}(u)$ can be interpolated from the table rather than rigorous computation. It is straightforward to show that

$$\sum_{j\in F}\tilde{P}_{i\to j}(u)=\sum_{j\in F}P_{i\to j}(u) \tag{22}$$

Therefore, the escape probability $P_{esc,i}(u)$ of the realistic temperature profile and material composition is still conserved through the approximation. In addition, by summarizing the right hand side of Eq. (19) over all sub-region *i* of the fuel, it can be shown that the set of $\tilde{P}_{i\to j}(u)$ also conserves the total reaction rate R of the whole fuel rod

$$\begin{aligned} R &= \sum_{j\in F}V_jQ_j(u)\sum_{i\in F}P_{j\to i}(u)+\sum_{i\in F}\sum_{k\in M}V_kP_{k\to i}(u)\Sigma_{p,k} = \\ &\sum_{j\in F}V_jQ_j(u)\sum_{i\in F}\tilde{P}_{j\to i}(u)+\sum_{i\in F}\sum_{k\in M}V_kP_{k\to i}(u)\Sigma_{p,k} = \tilde{R} \end{aligned} \tag{23}$$

Substituting $P_{i\to j}(u)$ in Eq. (20) with $\tilde{P}_{i\to j}(u)$ yields the following expression of flux

$$\phi_i(u)\approx\frac{1-P_{esc,i}(u)}{1-P_{esc,i}^{T_i,C_i}(u)}\sum_{j\in F}\frac{P_{i\to j}^{T_i,C_i}(u)}{\Sigma_{t,j}(u)}Q_j(u)+\sum_{k\in M}P_{i\to k}(u) \tag{24}$$

By defining $\bar{Q}_i(u)=\frac{\Sigma_{t,i}(u)}{1-P_{esc,i}^{T_i,C_i}(u)}\sum_{j\in F}\frac{P_{i\to j}^{T_i,C_i}(u)}{\Sigma_{t,j}(u)}Q_j(u)$ and replacing $\sum_{k\in M}P_{i\to k}(u)$ with $P_{esc,i}(u)$

$$\phi_i(u)=\frac{\bar{Q}_i(u)}{\Sigma_{t,i}(u)}\left[1-P_{esc,i}(u)\right]+P_{esc,i}(u) \tag{25}$$

Using the rational form of $P_{esc,i}(u) = \frac{\Sigma_{e,i}(u)}{\Sigma_{t,i}(u) + \Sigma_{e,i}(u)}$ ($\Sigma_{e,i}(u)$ should be energy dependent based on our investigation in Ref. [32]), the equation can be transformed into a form similar to the conventional equivalence theory

$$\phi_i(u) = \frac{\bar{Q}_i(u) + \Sigma_{e,i}(u)}{\Sigma_{t,i}(u) + \Sigma_{e,i}(u)} \tag{26}$$

Therefore, the quasi-1D slowing-down equation is defined as

$$\left[\Sigma_{t,i}(u) + \Sigma_{e,i}(u)\right]\phi_i(u) = \bar{Q}_i(u) + \Sigma_{e,i}(u) \tag{27}$$

This equation is actually in a 0-D form but 1-D information is embedded in $\bar{Q}_i(u)$ and $\Sigma_{e,i}(u)$. Determination of $\bar{Q}_i(u)$ includes two quantities, $Q_j(u)$ and $P_{i\to j}^{T_i,C_i}(u)$. Evaluation of $Q_j(u)$ is similar to the conventional homogeneous slowing-down calculation. A detailed description of efficient evaluation of $Q_j(u)$ can be found in Ref. [25]. The first flight collision probability is evaluated using Carlvik method [33] for the 1-D cylindrical geometry. A table of $P_{i\to j}$ versus total cross section is established before the resonance calculation for $P_{i\to j}^{T_i,C_i}(u)$ interpolation. Usually, 1000-2000 cross section points are sufficient to generate an accurate $P_{i\to j}$ table so the additional computing time is negligible.

In addition to $\bar{Q}_i(u)$, $\Sigma_{e,i}(u)$ is determined by rigorously evaluating $P_{esc,i}(u)$ using the realistic fuel temperature profile and material compositions in the 1-D cylindrical geometry. To incorporate the inter-pin shielding effect into $\Sigma_{e,i}(u)$, a straightforward approach could be to evaluate the equivalence cross section by 1-D cylindrical pin in infinite coolant and modify it by

the realistic Dancoff effect from ESSM calculation. Specifically, the CE equivalence cross section for infinite coolant is modified as

$$\Sigma_{e,i}(E) \approx \Sigma_{e,i}^{\inf}(E)\frac{\Sigma_{e,F,g}^{ESSM}}{\Sigma_{e,F,g}^{\inf}} \tag{28}$$

In this equation, $\Sigma_{e,i}^{\inf}(E)$ is the equivalence cross section of sub-region *i* evaluated using Carlvik method in 1-D cylindrical geometry with infinite coolant. $\Sigma_{e,F,g}^{ESSM}$ is the realistic equivalence cross section of the single fuel region obtained from ESSM. $\Sigma_{e,F,g}^{\inf}$ is the equivalence cross section of the single fuel region in 1-D cylindrical geometry with infinite coolant, calculated by the group-wise total cross section. To compute $\Sigma_{e,F,g}^{\inf}$, a few iterations are required between calculation of Carlvik equivalence cross section and interpolation from the RI tables. An alternative approach of using Eq. (28) could be to compute the Dancoff factor by comparing the fuel escape probability in the infinite coolant with the one in the realistic lattice, i.e.,

$$D_{F,g} = \frac{P_{e,F,g}^{ESSM}}{P_{e,F,g}^{\inf}} = \frac{\Sigma_{e,F,g}^{ESSM} \Big/ \left(\Sigma_{t,F,g}^{ESSM} + \Sigma_{e,F,g}^{ESSM}\right)}{\Sigma_{e,F,g}^{\inf} \Big/ \left(\Sigma_{t,F,g}^{\inf} + \Sigma_{e,F,g}^{\inf}\right)} \tag{29}$$

The Dancoff factor is in turn to modify $P_{esc,i}^{\inf}(u)$ and thus $\Sigma_{e,i}(E)$. Both approaches assume that the Dancoff effect is not dependent on energy so that the group-averaged factors are used for every point within each energy group. Although the definition of Dancoff factor in the second approach is conventionally used in Ref. [18,19], numerical experiments give slightly better results when the equivalence cross section is directly modified as Eq. (28). Therefore, the first approach is chosen for the quasi-1D model.

II.C. Correction based self-shielding method for annular fuel regions

The basic idea of the correction based self-shielding method for annular fuel regions is to compute the shielded cross sections by ESSM iteration with single mesh of the fuel region, and correct the multi-region effect by the factors obtained from the quasi-1D slowing-down calculation. The resonance interference and non-uniform temperature effects are also modeled by properly choosing the calculation conditions of the factors. The method is presented as follows:

Step 1. Solve ESSM using volume-averaged fuel temperature $\overline{T}$ and material composition for a single fuel region without resonance interference treatment. This step generates a set of shielded cross sections $\sigma_{iso,x,g,F}^{non-\mathrm{intf}}(\overline{T})$ (for isotope *iso*, energy group *g* and reaction channel *x*) incorporating inter-pin shielding effect (Dancoff effect) but without consideration of intra-pin effects or interference.

Step 2. Resolve the intra-pin and resonance interference effects by solving Eq. (27) for two sets of problems:

a. For the fuel mixture for each sub-region *i* of the fuel and realistic temperature distribution T_i, which produces shielded cross sections $\tilde{\sigma}_{iso,x,g,i}^{\mathrm{intf}}(T_i)$;

b. For each isolated isotope with single fuel region using uniform temperature $\overline{T}$ (conditions similar to Step 1), which produces shielded cross sections $\tilde{\sigma}_{iso,x,g,F}^{non-\mathrm{intf}}(\overline{T})$.

The ratio of shielded cross sections from problem **a** and **b** in Step 2 is used to correct the cross sections from Step 1, so the resultant shielded cross section is

$$\sigma_{iso,x,g,i}^{final}(T_i) = \sigma_{iso,x,g,F}^{non-\mathrm{intf}}(\overline{T}) \frac{\tilde{\sigma}_{iso,x,g,i}^{\mathrm{intf}}(T_i)}{\tilde{\sigma}_{iso,x,g,F}^{non-\mathrm{intf}}(\overline{T})} \tag{30}$$

The additional computation cost of the correction method compared to the conventional ESSM is to solve the quasi-1D slowing-down equation. Sub-step **a** in Step 2 requires a single slowing-down sweep for all the sub-regions of the fuel, while Sub-step **b** requires independent slowing-down sweeps for every resonance isotope of the fuel to exclude the interference effect. The computing condition of Sub-step **b** is similar to Step 1, except that the quasi-1D slowing-down model is used rather than the ESSM model. Therefore, by analogy with the heterogeneous RI tables described in Section II.A, a second set of heterogeneous RI tables is pre-computed using the quasi-1D slowing-down model and also parameterized by the background cross section. With the second set of RI tables, slowing-down calculation of Sub-step **b** in Step 2 can be substituted by table interpolation.

Surprisingly, another benefit is automatically gained when the second set of heterogeneous RI tables is used in the calculation of Sub-step **b**. As discussed earlier, the ESSM calculation in Step 1 introduces a bias on $\Sigma_{e,F,g}^{ESSM}$ and hence a bias on the shielded cross section $\sigma_{iso,x,g,F}^{non-\mathrm{intf}}(\overline{T})$ because of combining all the resonance isotopes as a whole absorber. However, since the biased $\Sigma_{e,F,g}^{ESSM}$ is also used in Sub-step **b** for interpolation of $\tilde{\sigma}_{iso,x,g,F}^{non-\mathrm{intf}}(\overline{T})$, the error introduced by this simplification is cancelled out to some extent because $\sigma_{iso,x,g,F}^{non-\mathrm{intf}}(\overline{T})$ and $\tilde{\sigma}_{iso,x,g,F}^{non-\mathrm{intf}}(\overline{T})$ are both monotonically increasing functions of the background cross section.

III. NUMERICAL VERIFICATIONS

The resonance self-shielding method for annular fuel regions was implemented and tested in the direct whole core neutron transport code DeCART [34]. Five PWR pin cell problems are selected for verification, including uniform and non-uniform fuel temperature profiles. MCNP calculations with CE cross section data were performed to provide the reference results.

III.A Code system

In comparison to the conventional 2-step (transport/diffusion) methodology where the first step is the generation of homogenized few group cross sections with a transport method and the second step is a global calculation with diffusion method, DeCART performs a direct transport calculation (2-D transport plus 1-D diffusion) using the realistic geometry, material composition and temperature profile of the reactor configuration and the number of energy groups may be as large as the number used for the lattice calculation in the 2-step method. The resonance self-shielding calculations are performed for every 2-D plane and the multi-group self-shielded cross sections are directly used in the whole core transport calculation without homogenization. Both the whole core transport calculation and the fixed source resonance calculations are performed with the MOC.

Two new modules are added to the original DeCART code, i.e., ESSM and correction factor generator. The ESSM is implemented in parallel to the subgroup method in DeCART to resolve the inter-pin shielding effect (Step 1 in Section II.C). The correction factor generator incorporates the quasi-1D slowing-down solver to produce the correction factors accounting for the intra-pin self-shielding details and resonance interference (Step 2 in Section II.C). The collision probability kernel is embedded in the slowing-down solver to provide the CE dependent equivalence cross sections. Once the ESSM iteration is complete, the module passes the group-wise equivalence cross sections to the correction factor generator for Dancoff adjustment (Eq. 28). The correction factors are then fed to the ESSM module to correct the self-shielded cross sections.

Fig. 2 depicts the data flow of the verification code system. The CE library is taken from SCALE 6.0 package [35] and the multi-group library is provided by Oak Ridge National Lab for use in the CASL project [36]. They are both processed by AMPX [37] from the raw nuclear data

of ENDF/B-VII.0 [38]. The CE data are employed when solving the slowing-down equations for the calculation of correction factors. The multi-group library structure consists of a total of 56 energy groups, in which 25 groups are defined as resonance groups (0.6eV~25keV). It has been mentioned that two sets of heterogeneous RI tables are generated. RI table Set 1 is processed by SCALE-CENTRM and AMPX-IRFfactor modules by performing the 2-D heterogeneous slowing-down calculation for the major resonance isotopes (U-238, U-235, Pu-239, Pu-240, Pu-241, Zr-91, Zr-96). This set of RI table has been loaded in the multi-group library for ESSM iteration. RI table Set 2 is generated by performing the quasi-1D slowing-down calculation and will be used for fast interpolation of the shielded cross section in Step 2-b of Section II.C. The subgroup parameters are also provided in the 56-group library, which are generated by the physical probability table approach and are consistent with RI table Set 1.

The MCNP5 code [39] is used to generate reference shielded cross sections for comparison with the new method. In order to produce CE libraries for MCNP use, a series of NJOY [40] modules are run to generate the ACE format data for every specific temperature appearing in the test problems. All the ACE data are prepared from ENDF/B-VII.0, which is the same source as the verification code system.

III.B Testing cases

The base test problem is a typical 2-D PWR pin cell in an infinite, uniform lattice. The fuel is 5% enriched with the pellet outside radius of 0.4096cm. The pin pitch is 1.26cm. The UO_2 fuel pellet is subdivided into 10 equal-volume annuli. Five cases with different temperature profiles in the fuel pellet are tested, as shown in Table I. The temperatures in regions other than fuel are all set to 600K. Cases 1-3 are uniform temperature cases and Case 4-5 are non-uniform temperature

cases in which the ring-wise temperatures are integrated from a parabolic temperature distribution with volume average values of 900K and 1200K, respectively.

III.C Numerical results

In this subsection, the notation 'ESSM^{OLD}' refers to the conventional ESSM with simple multi-region extension. 'ESSM^{CRT}' refers to the proposed correction method. In addition to ESSM calculation, the subgroup method with special treatment for non-uniform temperature distribution [22] is also included for comparisons. All three methods are run with the same spatial discretization and MOC ray options (4/24/0.01 for polar/azimuthal/ray spacing). ESSM^{OLD} and the subgroup method use the Bondarenko iteration for treatment of resonance interference. The MCNP reference solution is calculated with 600 active cycles and 20000 histories per cycle to make a total of 12 million neutron histories. As a result, the standard deviation of reaction rates for every reaction channel and every resonance energy group is below 1%, and the standard deviations of reaction rates over the resonance energy range (0.625eV-25keV) for U-238 absorption, U-235 absorption and U-235 fission are 0.04%, 0.03% and 0.03%, respectively.

Table II compares the spatially dependent shielded cross sections for U-238 in Group 34 (6.5eV-6.88eV) for the three methods with MCNP. Since this is the major resonance of U-238, a strong spatial self-shielding is seen from the reference solution, e.g., the shielded cross section for the outermost ring is almost three times that for the innermost ring for Case 1. Interestingly, the shielded cross section of Group 34 is not monotonically increasing from the fuel center to the surface for the uniform temperature cases. The values become a bit larger towards the center for the innermost four or five rings. This can be explained by comparing the CE fluxes of every fuel ring, in which the fluxes of the inner rings are relatively flatter about energy than those of the middle rings due to the strong spatial shielding. The relative errors show that ESSM^{OLD} is unable

to correctly produce the spatially shielded cross sections. For all the five cases, it underestimates the cross sections of the surface ring and overestimates those of the inner rings. Compared to $ESSM^{OLD}$, the subgroup method performs better for the surface ring, but still, has large discrepancies for the inner rings. The shielded cross sections generated by $ESSM^{CRT}$ compare favorably with MCNP results, showing an order of magnitude in relative error compared to the $ESSM^{OLD}$ and subgroup method. The agreement of non-uniform temperature cases is on the same order as the agreement with the uniform temperature cases, indicating the effectiveness of the collision probability approximation in Eq. (21). The agreement of other resonance groups is similar to Group 34 and thus the results are not repeated.

Table III shows the spatially dependent absorption cross sections of U-235 for Group 22 (116.0eV-117.5eV) where the resonance interference due to U-238 is significant. Because the spectra are dominated by U-238 absorption resonances, the regular shielding behavior that the shielded cross section tends to the peak at the fuel surface is not seen in this group for U-235. $ESSM^{OLD}$ and the subgroup method using Bondarenko iteration fail to model the resonance interference, so large discrepancies are observed across all the rings of the fuel rod. Since $ESSM^{CRT}$ employs CE cross sections explicitly for interference correction, the errors of shielded cross sections are reduced to less than 1% for most sub-regions.

Multiplying the shielded cross sections by the group fluxes gives the reaction rate per atom in different rings of the fuel. In order to rule out the flux discrepancies between MCNP and DeCART due to the sources other than resonance calculation, instead of directly using the MCNP reaction rates as the reference solution, the shielded cross sections tallied from MCNP are fed to DeCART to calculate the reference reaction rates. Figures 3-7 compare the errors of U-238 absorption rates for the five cases using $ESSM^{OLD}$, subgroup method, and $ESSM^{CRT}$ relative to the reference results of DeCART (MCNP XS). Two resonance groups are considered, Group 34 (6.5eV-6.88eV), Group 22 (116.0eV-117.5eV), as well as the whole resonance energy range

(0.625eV-25keV). For $ESSM^{OLD}$, a 15%-20% underestimation of total resonance absorption rate at the outmost ring is observed for all the cases. As plutonium buildup tends to peak at the fuel surface, this bias could significantly undermine the accuracy of a multi-region depletion calculation. The errors of reaction rates for subgroup method are still significant for a single resonance group, but become smaller over the whole resonance range. Because of the lack of a theoretical foundation for treating a non-uniform temperature profile with the subgroup method, the discrepancies of non-uniform temperature cases are somewhat larger than the uniform temperature cases. Of the three methods, $ESSM^{CRT}$ produces the best spatial distribution of the reaction rates, both for a single group and for the whole resonance range. The largest difference over the whole resonance range of all the annuli is only 1.3%.

Previous comparisons have shown that resonance interference effect is more important for U-235 than the spatial shielding effect, so the integrated absorption and fission rates of U-235 over the fuel pallet are compared for all resonance groups in Fig. 8 and Fig. 9 (Case 1 and Case 4 are arbitrarily selected and other cases have similar results). The reference absorption and fission rates are shown on the upper side and the relative errors using $ESSM^{OLD}$, the subgroup method and $ESSM^{CRT}$ are compared on the lower side. $ESSM^{OLD}$ and the subgroup method treat the resonance interference by Bondarenko iteration, which is unable to produce the correct reaction rates for U-235 at the energy ranges where there are large resonances of U-238 (i.e. 6.67eV, 21eV and so on). Since the overlap condition of the resonances between U-235 and U-238 is arbitrary at different energy ranges, the errors of $ESSM^{OLD}$ and subgroup method can be positive or negative. The reaction rates calculated by $ESSM^{CRT}$ have good agreement with the reference results. The maximum error is 3.8%, compared to more than 100% by Bondarenko iteration.

Table IV compares the effective multiplication factors and the total reaction rates of U-235 and U-238 in the resonance energy range (0.625eV-25keV). For these runs, DeCART was performed with MCNP tallied cross sections to calculate the reference results. It is not surprising

that $ESSM^{OLD}$ and the subgroup method show larger discrepancies for the U-238 absorption rates, consistent with earlier results with the spatial shielding. Although very large differences were seen in the analysis of U-235 group-wise reaction rates, the total absorption and fission rates over the whole resonance energy range are not that bad for $ESSM^{OLD}$ and subgroup method. This is probably due to the error cancellation. For some cases, the U-235 fission rates from $ESSM^{CRT}$ are comparable to results from $ESSM^{OLD}$ or the subgroup method, but those errors are already within a few standard deviations of MCNP calculations. Overall, $ESSM^{CRT}$ gives the best agreement of eigenvalues for all the five cases.

Regarding the treatment of non-uniform temperature in $ESSM^{CRT}$, Step 1 and Step 2-b need an average temperature over the fuel rod. The volume-averaged temperature is simply chosen to obtain the foregoing results for Case 4 and 5. As mentioned in the introduction section, various approaches were developed to determine the average temperature (effective temperature), e.g., chord averaged temperature. In order to show the adequacy of using volume-averaged in the correction model, Case 4 and Case 5 are rerun with the volume-averaged temperature manually varied by $\pm$50K and $\pm$100K. The variation range of the temperature can be viewed as possible effective temperatures elaborately calculated by the models mentioned in Ref. [21]. Table V shows that the eigenvalues calculated by $ESSM^{CRT}$ have almost no change with variation of the average temperature. The bias introduced by the deviation of the average temperature from the true effective temperature is canceled out during the correction of shielded cross sections in Eq. (30). The volume-averaged scheme is therefore sufficient for the correction model.

As the CE slowing-down calculation is involved in the correction model, it is crucial to analyze the computing resources required for the method. Table VI compares the computing time and memory usage of $ESSM^{OLD}$, subgroup method and $ESSM^{CRT}$. Case 2 (uniform 900K) and Case 4 (parabolic with 900K average) are selected for the test. To show the impact of number of the rings, Case 2 is varied by dividing the fuel region into 3, 6 and 10 equal-volume rings. The

computing time of $ESSM^{OLD}$ and subgroup method is primarily determined by the number of fixed source problems to be solved. The average number of iteration to converge equivalence cross sections for each group in ESSM is about three to five, which is in the same order of the number of subgroup levels. However, the subgroup method distributes the resonance isotopes into several resonance categories for the fixed source calculations, which leads to more resonance computing time for the subgroup method. Comparing $ESSM^{OLD}$ and $ESSM^{CRT}$ for the uniform temperature case, the resonance calculation time increases with the number of rings, and $ESSM^{CRT}$ cost additional 4.5% , 15% and 21% time on resonance calculation for the 3, 6 and 10 ring cases, respectively. For the non-uniform temperature case, the resonance calculation time has risen by 84%. Since only a few discrete temperatures are available in the AMPX CE library (293K, 600K, 900K, 1200K and 2400K), the CE cross section should be interpolated on the fly of the slowing-down equation, which is one reason why larger increase of time is seen for the non-uniform temperature case. Another reason is the increasing size of energy mesh for slowing-down calculation due to the temperature differences of fuel regions. Even so, the total computing time only rises by about 10%, a modest increase. The memory demand of the slowing-down calculation depends primarily on the number of isotopes and the range of temperatures in the problem. Since the slowing-down calculations for the fuel pins are decoupled, the memory requirement for the model does not increase with the geometrical size of the problem. This also makes the model easy to be implemented in parallel.

IV. CONCLUSIONS

A correction based resonance self-shielding method is developed that allows annular subdivision of the fuel rod. The method incorporates CE slowing-down calculations to account for the radial variation of the self-shielded cross sections, resonance interference, and a non-

uniform temperature distribution within the fuel. Starting from the collision probability form of the integral transport equation, an efficient quasi-1D slowing-down equation is derived. The proposed method performs conventional ESSM iteration without subdivision of the fuel rod to capture the inter-pin shielding effect. Correction factors are obtained by comparing the shielded cross sections of the subdivided fuel rod with a single region of the fuel. These shielded cross sections are efficiently computed by solving the quasi-1D slowing-down equation. By properly choosing the computing conditions of shielded cross sections, the resonance interference and non-uniform temperature effect are accounted for by the correction factors.

Numerical results show that the correction method is capable of resolving the spatially dependent self-shielding of fuel annuli. Compared to the conventional ESSM, the error of U-238 absorption rate over the resonance energy range for the outmost ring is reduced from 15%-20% to less than 1% by the correction model. The accuracy of U-235 group-wise reaction rates is significantly improved by properly correcting the resonance interference. The eigenvalues and overall reaction rates of U-238 and U-235 are all improved by the correction method. The method is not sensitive to the temperature averaging scheme so that the simple volume average is sufficient to perform the task. The additional computing time is negligible for the uniform temperature case, and a modest 10% increase over the total calculation time for the non-uniform temperature case. The memory usage of the method is acceptable and does not increase with the geometrical size.

The accurate spatially shielded cross sections within the fuel rod will be important for the determination of the fuel burnup distribution. This will benefit the thermal hydraulic calculation as the fuel conductivity is very sensitive to burnup. Also, the plutonium build-up at the fuel surface requires careful concern. The so called plutonium ‘rim effect' can occur at very high burnup and the thermal conductivity of the fuel can be significantly reduced in the rim zone. This phenomenon could be modeled only if the plutonium build-up is accurately estimated, which in

turn depends on the U-238 absorption rate near the fuel surface. In addition to the burnup, the distribution of the heat generation and fission product generation can also be improved by properly determining the spatially dependent shielded cross sections.

ACKNOLEDGEMENT

This research was supported by the Consortium for Advanced Simulation of Light Water Reactors (http://www.casl.gov), an Energy Innovation Hub (http://www.energy.gov/hubs) for Modeling and Simulation of Nuclear Reactors under U.S. Department of Energy Contract No. DE-AC05-00OR22725.

The first author wishes to express his gratitude to Professor Han Gyu Joo of Seoul National University for his correction suggestion of some plots.

REFERENCE

1. F. Leszczynski, "Neutron Resonance Treatment with Details in Space and Energy for Pin Cells and Rod Clusters," *Ann. Nucl. Energy*, **14**, 589 (1987).
2. M. L. Williams and M. Asgari, "Computation of Continuous-Energy Neutron Spectra with Discrete Ordinates Transport Theory," *Nucl. Sci. Eng*., **121**, 173 (1995).
3. K. S. Kim and S. G. Hong, "The Method of Characteristics Applied to Solving Slowing Down Equation to Estimate the Self-shielded Resonance Cross Sections with an Explicit Geometrical Effect," *Ann. Nucl. Energy*, **38**, 438 (2011).
4. K. S. Kim and M. L. Williams, "The Method of Characteristics for 2-D Multigroup and Pointwise Transport Calculations in SCALE/CENTRM," *Proc. PHYSOR-2012*, Knoxville, TN, April 15-20 (2012).

5. Z. Zhong, T. J. Downar and Y. Xu, "Continuous-Energy Multidimensional SN Transport for Problem-Dependent Resonance Self-Shielding Calculations," *Nucl. Sci. Eng*., **154**, 190 (2006).
6. I. I. Bondarenko, *Group Constants for Nuclear Reactor Calculations*, Consultants Bureau, New York (1964).
7. R. J. J. Stamm'ler and M. J. Abbate, *Methods of Steady-state Reactor Physics in Nuclear Design*, Academic Press, London (1983).
8. J. R. Askew, F. J. Fayers, and P. B. Kemshell, "A General Description of the Lattice Code WIMS," *J. British Nucl. Energy Soc*., **5**, 564 (1966).
9. L. B. LEVITT, "The Probability Tables Method for Treating Unresolved Neutron Resonances in Monte-Carlo Calculations," *Nucl. Sci. Eng.*, **49**, 450 (1972).
10. D. E. Cullen, "Application of the Probability Table Method to Multigroup Calculations of Neutron Transport," *Nucl. Sci. Eng.* **55**, 387 (1974).
11. A. Hébert, "A Review of Legacy and Advanced Self-Shielding Models for Lattice Calculations," *Nucl. Sci. Eng.*, **155**, 310 (2007).
12. S. G. Hong and K. S. Kim, "Iterative Resonance Self-Shielding Methods Using Resonance Integral Table in Heterogeneous Transport Lattice Calculations," *Ann. Nucl. Eng.*, **38**, 32 (2011).
13. M. L. Williams and K. S. Kim, "The Embedded Self-shielding Method," *PHYSOR-2012*, Knoxville, TN, April 15-20, (2012).
14. M. L. Williams, "Correction of Multigroup Cross Sections for Resolved Resonance Interference in Mixed Absorbers," *Nucl. Sci. Eng*., **83**, 37 (1983).
15. K. S. Kim and S. G. Hong, "A New Procedure to Generate Resonance Integral Table with an Explicit Resonance Interference for Transport Lattice Codes", *Ann. Nucl. Energy.*, **38**, 118 (2011).

16. Z. Gao, Y. Xu and T. J. Downar, “The Treatment of Resonance Interference Effects in the Subgroup Method,” *Ann. Nucl. Energy.*, **38**, 995 (2011).

17. K. Smith and B. Forget, “Challenges in the Development of High-Fidelity LWR Core Neutronics Tools,” *Proc. M&C-2013*, Sun Valley, Idaho, May 5-9 (2013).

18. C. Stoker and Z. Weiss, “Spatially Dependent Resonance Cross Sections in a Fuel Rod,” *Ann. Nucl. Energy.*, **23**, 765 (1996).

19. M. Williams and R. Raharjo, “Space-Dependent Resonance Self-shielding,” *Nucl. Sci. Eng.*, **126**, 19 (1997).

20. H. Matsumoto, M. Ouisloumen and T. Takeda, “Development of Spatially Dependent Resonance Shielding Method,” *J. Nucl. Sci Technol.*, **42**, 688 (2005).

21. W. J. M. de Kruijf and A. J. Janssen, ‘‘The Effective Temperature to be Used for Calculating Resonance Absorption in a $^{238}UO_2$ lump with nonuniform temperature profile,’’ *Nucl. Sci. Eng.*, **123**, 121 (1996).

22. H. G. Joo, B. S. Han, C. H. Kim and K. S. Kim, “Implementation of Subgroup Method in Direct Whole Core Transport Calculation Involving Nonuniform Temperature distribution,” *Proc. M&C-2005*, Palais des Papes, Avignon, France, September 12-15 (2005).

23. C. A. Wemple, R. J. J. Stamm’ler and A. A. Ferri, “Improved Temperature-Dependent Resonance Treatment in HELIOS-1.9,” *Trans. Am. Nucl. Soc.*, **96**, 657 (2007)

24. K. S. Kim and Mark L. Williams, "Preliminary Assessment of Resonance Interference Treatment by Using 0-D Slowing Down Calculation in the Embedded Self-Shielding Method," *Trans. Am. Nucl. Soc.*, **107**, 1128 (2012)

25. Y. Liu, W. R. Martin, K. S. Kim and M. L. Williams, “Modeling Resonance Interference by 0-D Slowing-down Solution with Embedded Self-shielding Method,” *Proc. M&C-2013*, Sun Valley, Idaho, May 5-9 (2013).

26. R. Goldstein and E. R. Cohen, “Theory of resonance absorption of neutrons,” *Nucl. Sci. Eng.*,

13, 132 (1962).

27. R. E. MacFarlane and D. W. Muir, “NJOY99.0 code system for producing pointwise and multigroup neutron and photon cross sections from ENDF/B Data,” *Report PSR-80/NJOY99.0*, Los Alamos National Laboratory, New Mexico (2000).
28. B. Fredin, U. Decher, A. Jonsson, A. Ferri and R. J. J. Stamm’ler, “Processing and Application of ENDF/B-VI in LWRs: Critical Experiments”, *Trans. Am. Nucl. Soc.*, **73**, 419 (1995).
29. R. J. J. Stamm’ler, et al., *HELIOS Methods*, Studsvik Scandpower (2003).
30. K. S. Kim, C. C. Lee, M. H. Chang and S. Q. Zee, “Monte Carlo resonance treatment for the deterministic transport lattice code”. *J. Korean Nucl. Soc.*, **35**, 581 (2003).
31. H. G. Joo, G. Y. Kim and L. Pogosbekyan, “Subgroup weight generation based on shielded pin-cell cross section conservation,” *Ann. Nucl. Energy*, **36**, 859 (2009).
32. Y. Liu, W. R. Martin, M. L. Williams and K. S. Kim, “Modeling Spatial Dependence of Resonance Self-shielding Effects Including Resonance Interference and Temperature Distribution,” *Trans. Am. Nucl. Soc*., **109**, 800 (2013).
33. I. Carlvik, “A Method for Calculating Collision Probabilities in General Cylindrical Geometry and Applications to Flux Distributions and Dancoff Factors,” *Proc. Int. Conf. Peaceful Uses of Atomic Energy in Geneva*, **2**, 225, United Nations, New York (1965).
34. H. G. Joo, J. Y. Cho, K. S. Kim, C. C. Lee, M. H. Chang and S. Q. Zee, “Methods and Performance of a Three-Dimensional Whole-Core Transport Code DeCART,” *Proc. PHYSOR-2004*, Chicago, IL, April 25-29 (2004).
35. S. M. Bowman, "SCALE 6: Comprehensive Nuclear Safety Analysis Code System," *Nucl. Technol*. **174**, 126 (2011).
36. W. R. Martin, “The CASL Nuclear Energy Modeling and Simulation Energy Innovation Hub – Panel”, ANS Winter Meeting 2010, Las Vegas, Nevada, November 7-11, 2010.

37. M. E. Dunn and N. M. Greene, “AMPX-2000: A Cross-Section Processing System for Generating Nuclear Data for Criticality Safety Applications,” *Trans. Am. Nucl. Soc*., **86**, 118 (2002).

38. M. B. Chadwick, et al., “ENDF/B-VII.0: Next Generation Evaluated Nuclear Data Library for Nuclear Science and Technology,” *Nucl. Data Sheets*, **107**, 2931 (2006).

39. X-5 Monte Carlo Team, “MCNP-A General Monte Carlo N-Particle Transport Code, Version 5”, LA-UR-03-1987, Los Alamos National Laboratory (2000).

40. R. E. MacFarlane and D. W. Muir, “NJOY99.0 Code System for Producing Pointwise and Multigroup Neutron and Photon Cross Sections from ENDF/B Data,” Report PSR-480/NJOY99.0, Los Alamos National Laboratory, New Mexico (2000).